DOI: 10.1002/eji.201848001 Eur. J. Immunol. 2019. 49: 954–965

European Journal of Immunology

New Technology

Research Article

Accelerated thymopoiesis and improved T-cell responses in HLA-A2/-DR2 transgenic BRGS-based human immune system mice

Guillemette Masse-Ranson[1,2,3], Mathilde Dusséaux[1,2], Oriane Fiquet[1,2], Sylvie Darche[1,2], Maud Boussand[1,2], Yan Li[1,2], Silvia Lopez-Lastra[1,2], Nicolas Legrand[4], Erwan Corcuff[4], Antoine Toubert[5,6], Mireille Centlivre[3], Timothée Bruel[3,7,8], Hergen Spits[9], Olivier Schwartz[3,7,8], Yves Lévy[3,10,11], Hélène Strick-Marchand[1,2] and James P. Di Santo[1,2]

[1] Inserm U1223, Paris, France
[2] Innate Immunity Unit, Institut Pasteur, Paris, France
[3] Vaccine Research Institute, Créteil, France
[4] genOway, Fontenay-aux-Roses, France
[5] Laboratoire d'Immunologie et d'Histocompatibilité, Hôpital Saint-Louis, Paris, France
[6] INSERM UMR1160, Institut Universitaire d'Hématologie, Paris, France
[7] Virus and Immunity Unit, Institut Pasteur, Paris
[8] CNRS-URA 3015, Paris, France
[9] AMC, Amsterdam, The Netherlands
[10] Inserm U955, Equipe 16, Créteil, France
[11] AP-HP, Hôpital Henri-Mondor Albert-Chenevier, Service d'Immunologie Clinique et Maladies Infectieuses, Créteil, France

Human immune system (HIS) mouse models provide a robust in vivo platform to study human immunity. Nevertheless, the signals that guide human lymphocyte differentiation in HIS mice remain poorly understood. Here, we have developed a novel Balb/c *Rag2*$^{-/-}$ *Il2rg*$^{-/-}$ *Sirpa*^{NOD} (BRGS) HIS mouse model expressing human HLA-A2 and -DR2 transgenes (BRGSA2DR2). When comparing BRGS and BRGSA2DR2 HIS mice engrafted with human CD34^{+} stem cells, a more rapid emergence of T cells in the circulation of hosts bearing human HLA was shown, which may reflect a more efficient human T-cell development in the mouse thymus. Development of CD4^{+} and CD8^{+} T cells was accelerated in BRGSA2DR2 HIS mice and generated more balanced B and T-cell compartments in peripheral lymphoid organs. Both B- and T-cell function appeared enhanced in the presence of human HLA transgenes with higher levels of class switched Ig, increased percentages of polyfunctional T cells and clear evidence for antigen-specific T-cell responses following immunization. Taken together, the presence of human HLA class I and II molecules can improve multiple aspects of human B- and T-cell homeostasis and function in the BRGS-based HIS mouse model.

Keywords: Animal models · Humanized mice · Lymphocyte development

Additional supporting information may be found online in the Supporting Information section at the end of the article.

Correspondence: Prof. James P. Di Santo
e-mail: james.di-santo@pasteur.fr

Introduction

Human immune system (HIS) mice provide a valuable small animal model to study human immune responses following infection, vaccination, or in response to malignantly transformed cells. HIS mice are generated following engraftment of $CD34^+$ hematopoietic stem cells (HSC) in irradiated immunodeficient hosts and this represents a simple approach to reconstitute a majority of adult hematopoietic lineages [1–3]. The resulting HIS mice harbor a wide variety of human immune cells (B, T, NK, myeloid) that are present in diverse organs (spleen, bone marrow, thymus, liver, lung, mesenteric lymph nodes, and to a lesser extent in the gut) [2, 4, 5]. Finally, HIS models generate stable hematopoietic reconstitution that can last for > 6 months. Nevertheless, HIS mice do not perfectly model human hematopoiesis and fail to recapitulate critical aspects of human immune responses (reviewed in [6]). For example, antigen-specific B- and T-cell responses are suboptimal in most HIS mice, which may reflect the fact that human lymphocytes are not properly "educated" in the context of murine HLA within the stromal microenvironment. This lack of cognate interaction might be responsible for the impaired T-cell specific responses and poor B-cell differentiation (reduced Ig class switching) that have been described in HIS mice [4, 7–9].

Genetic modifications such as transgenes, knock-in or knockout mutations have been used to create modified HIS models with improved functionality [10–19]. As antigen receptors and MHC molecules have coevolved during evolution, it could be expected that transgenic expression of human HLA molecules followed by engraftment with HLA-matched HSC should generate a HIS model with improved development of HLA-restricted human T cells. In HLA-A2 transgenic NSG (NOD $Prkdc^{scid}$ $Il2rg^{tm1wjl}$) mice, antigen-specific $CD8^+$ T-cell responses against viral antigens or vaccines was improved [10–15, 17]. NOD *Rag2*$^{-/-}$ *Il2rg*$^{-/-}$ hosts containing a HLA-DR4 transgene (DRAG mice; hybrid HLADR0101α1/I-E^d, regulated by the mouse I-E^d promoter) reconstituted with matched HSCs, were shown to develop more T cells, especially $CD4^+$ T cells, sustained higher levels of human natural antibodies (IgM and IgG), and elicited efficient antibody responses to tetanus toxin vaccination [11]. HIS mice expressing both class I (HLA-A2) and class II (HLA-DR4) MHC transgenes (DRAGA mice) generated $CD8^+$ specific T cells and cytotoxicity upon immunization, mounting influenza-specific antibody responses [20], that were not observed in HLA-A2 only HIS mice (HLA-A2.1α 1α 2/H-$2D^b$) [21].

In the present study, we generated a novel HLA-transgenic HIS model based on Balb/c *Rag2*$^{-/-}$ *Il2rg*$^{-/-}$ *Sirpa*^{NOD} (Balb/c *Rag2*^{tm1Fwa} *Il2rg*^{tm1Cgn} *Sirpa*^{NOD}; BRGS hosts [2] with HLA-A2 and HLA-DR2 transgenes (BRGSA2DR2). We found that BRGSA2DR2 hosts engrafted with matched HSC display a more rapid reconstitution of T-cell subsets, in particular $CD8^+$ T cells, as well as higher levels of class-switched IgG and improved generation of vaccine-induced antigen-specific T cells. BRGSA2DR2 HIS mice extend the arsenal of HLA transgenic HIS mouse models that can be used as preclinical tools to assess immunogenicity of human vaccine candidates.

Results

BRGSA2DR2 HIS mice show accelerated kinetics of human immune cell engraftment

To assess the impact of transgenic expression of human MHC class I and class II molecules on human lymphocyte development in an immunodeficient Balb/c background, HLA-A2 'HHD' (encoding a hybrid HLA-A2.1/H-$2D^b$ α chain covalently linked to human β2-microglobulin; [22]) and HLA-DR2 (DRA*0101 and DRB1*1501 under control of the mouse MHC II promoter; [23]) transgenes were extensively backcrossed to BRGS mice [2] yielding BRGSA2DR2 hosts. HIS mice were generated in BRGS or BRGSA2DR2 neonatal recipients with HLA-$A2^+DR2^+$ $CD34^+$ HSC as previously described [16, 24–28] and composition of human $CD45^+$ hematopoietic cell subsets in the blood of engrafted HIS mice was assessed at 8 and 12 weeks postgraft (wpg) (Fig. 1A, B). Compared with non-HLA transgenic BRGS HIS mice, BRGSA2DR2 HIS mice showed more T cells in the blood at 8 wpg with a higher percentage of $CD8^+$ T cells (Fig. 1A). This difference persisted at 12 wpg. The early generation of T cells resulted in a higher frequency of $CD45^+$ cells in BRGSA2DR2 HIS mice at 8–10 wpg (Fig. 1B). B cells emerge in the blood before T cells in many HIS mouse models [4], and BRGS HIS mice are no exception: B cells outnumber T cells by 20 to 100-fold in the early postengraft period (Fig. 1C). Expression of human HLA class I and class II transgenes in the host equilibrated the B/T ratio in the blood at all-time points assessed (Fig. 1C). Finally, BRGS HIS mice show a marked bias toward generation of $CD4^+$ T cells at 12 wpg with an elevated CD4/CD8 ratio; this bias is not observed in BRGSA2DR2 HIS mice that maintain a normal CD4/CD8 ratio (Fig. 1D). Together, these results demonstrate accelerated kinetics and more balanced composition of human T- and B-cell development in BRGSA2DR2 HIS mice.

Analysis of human thymopoiesis in BRGSA2DR2 HIS mice

We next assessed the impact of human HLA-A2 and -DR2 transgenes on human intrathymic T-cell development in the BRGS HIS mouse model. Thymocytes were isolated and phenotyped for their major subsets ($CD4^-CD8^-$ "double negative" DN, $CD4^+CD8^+$ "double positive" DP, $CD4^+$ "single positive" CD4SP and $CD8^+$ "single positive" CD8SP) at 8 and 16 wpg. When comparing CD4 versus CD8 thymocytes, BRGSA2DR2 HIS mice showed more DP cells, a higher frequency of CD8SP and a reduction in DN cells at 8 wpg (Fig. 2A, B). Within the mature thymic $CD3^+$ T cells, HLA expression had an important impact on CD8SP development (Fig. 2A). Concerning absolute numbers of cells, thymi from BRGSA2DR2 HIS mice harbored more human hematopoietic cells that was largely due to increased numbers of mature $CD3^+$ T cells (Fig. 2C) including CD4SP and CD8SP thymocytes that were significantly increased (Fig. 2D). Taken together, the analysis of intrathymic

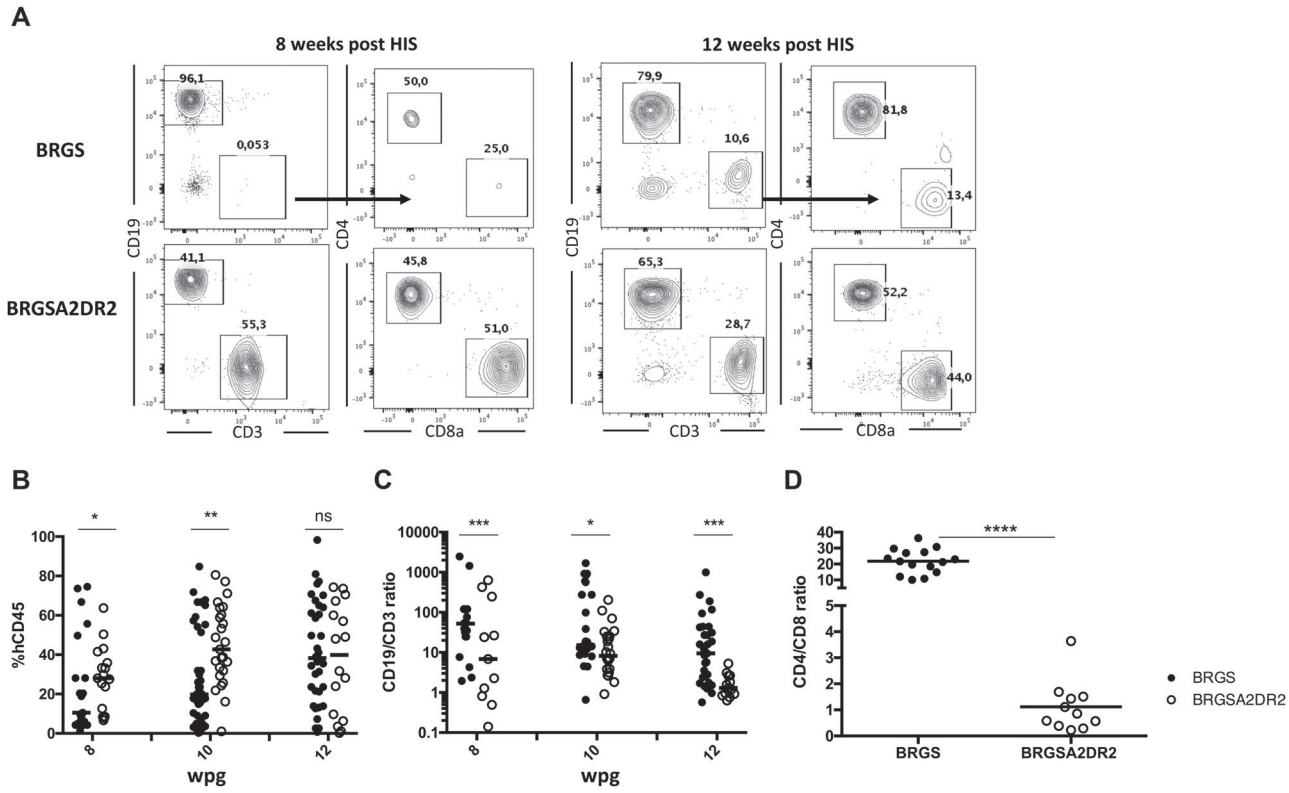

Figure 1. Kinetics of human cell reconstitution in the blood of BRGS versus BRGSA2DR2HISmice. (A) Representative flow cytometry immunephenotypic analysis of hCD45$^+$ blood cells at 8 weeks and 12 weeks post graft (wpg) in humanized BRGS versus BRGS HLA-A*02-HHD class I and HLA-DRB1*15 class II transgenic mice (BRGSA2DR2) reconstituted with HLA-A*02$^+$ HLA-DRB1*15$^+$ HSCs. (B) Analysis of hCD45$^+$ cells using the hCD45% × 100/ (hCD45% + mCD45%) formula (B) or CD19/CD3 ratio (C) over time (wpg) in BRGS (full circle) and BRGSA2DR2 (open circle). (D) Comparison of the CD4/CD8 ratios in both models at 12 wpg. Each dot represents one mouse and data are representative from at least five independent experiments (14–34 mice in each group).

T-cell development in BRGSA2DR2 HIS mice suggest that the earlier emergence of peripheral T cells in the early postgraft period is due to enhanced and accelerated thympoiesis following selection on human HLA.

B-cell development in BRGSA2DR2 HIS mice

HIS mice develop a diverse repertoire of Ig$^+$ B cells in the BM and spleen [4, 9]. Comparing BRGS and BRGSA2DR2 HIS mice, we found that absolute numbers of splenic CD19$^+$CD20$^+$ B cells and IgM$^+$IgD$^+$ mature B cells were similar at 8 wpg (Fig. 3A, B) suggesting that early emergence of mature T cells from the thymus did not affect B-cell homeostasis at this time. Splenic B cells at 8 wpg showed an immature, transitional phenotype (IgM$^+$IgD$^-$CD10^{hi}CD38^{hi}; Fig. 3B) as observed previously [4, 18, 29], and CD27$^+$ memory B cells were rare in both BRGS and BRGSA2DR2 models (Fig. 3A, B).

A different picture emerged when the B-cell analysis was performed at 16 wpg. Absolute numbers of splenic B cells were decreased in BRGSA2DR2 HIS mice and IgM$^+$IgD$^+$ cells were notably diminished, whereas the frequency of CD27$^+$ memory B cells was increased (Fig. 3A, B). Moreover, transitional CD38$^+$ B cells were less frequent in the BM of BRGSA2DR2 HIS mice at 16 wpg (Fig. 3B). These results suggest enhanced B-cell activation and switch of naïve IgM$^+$ B cells to IgG-producing progeny in BRGSA2DR2 HIS mice. While plasma cells (phenotype) were not detected in either HIS mouse model (Fig. 3C), we found that steady-state levels of IgG were markedly enhanced in BRGSA2DR2 HIS mice starting at 12 wpg (Fig. 3D). The evolution of B-cell homeostasis may be the result of enhanced T-B cooperation available in BRGSA2DR2 HIS mice.

Impact of HLA expression on peripheral T-cell subsets in BRGSA2DR2 HIS mice

We further characterized the peripheral T-cell compartment in these two HIS models through analysis of activated phenotype (CD45RO$^+$ CD45RA$^-$), and further activation states using CD45RA$^+$ CD27$^+$ naïve (N), CD45RA$^-$ CD27$^+$ central memory (CM), CD45RA$^-$ CD27$^-$ effector memory (EM), and CD45A$^+$ CD27$^-$ effector memory T cells (EMRA) in CD4$^+$ and CD8$^+$ compartments. Representative staining patterns are shown in Fig. 4A. No significant differences in absolute numbers of splenic CD4$^+$ or CD8$^+$ T cells were observed at 16 wpg (Fig. 4B). Similar

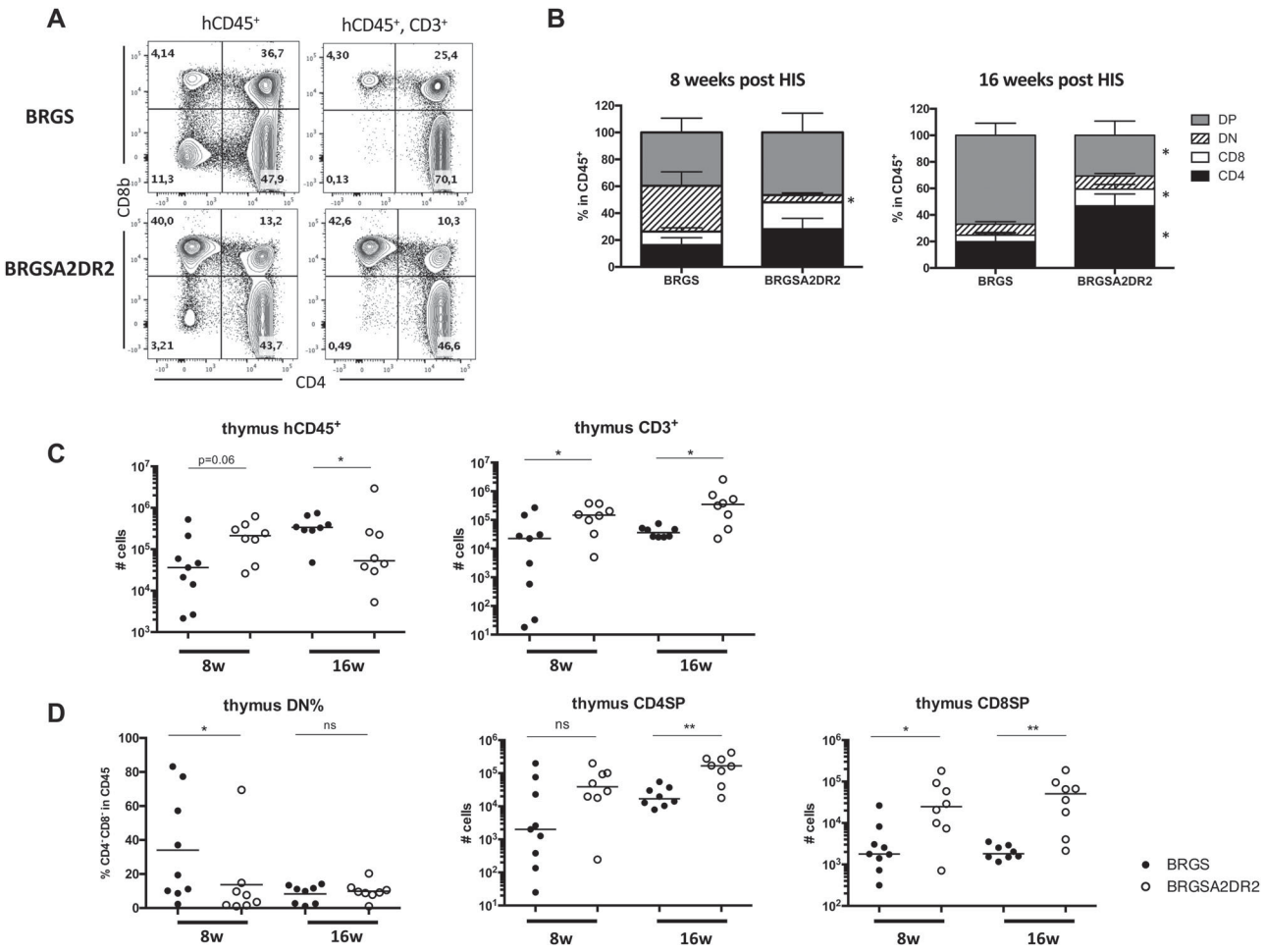

Figure 2. Human thymopoiesis in BRGS versus BRGSA2DR2 HIS mice. (A) FACS analysis showing the human $CD4^+$ and $CD8^+$ T-cell reconstitution in the thymus at 8 wpg in single, alive, $hCD45^+$ or $hCD45^+$ $CD3^+$ cells. (B) Bar graph showing the percentages of each population in the thymus in the $hCD45^+$ gate (DN: double negative $CD4^-CD8^-$, DP: double positive $CD4^+$ $CD8^+$, $CD8^+$ simple positive and $CD4^+$ simple positive) in both models at 8 and 16 wpg. Statistical analysis (*p*-value summary) comparing the frequency of each subset from the two models are on the side of the bar graph. (C) Total human $CD45^+$ and $CD3^+$ cellularity in the thymus of BRGS (full symbols) and BRGSA2DR2 (open symbols) reconstituted with HLA-A*02$^+$ HLA-DRB1*15$^+$ HSCs at 8 and 16 wpg. (D) Analysis of the percent age of double negative (DN) cells in the $CD45^+$ population and absolute numbers of $CD3^{hi}$ $CD8^+$ and $CD3^{hi}$ $CD4^+$ SP in the thymus of both models at 8 and 16 wpg. Each dot represents one mouse (8–9 mice per group) and data are representative from three experiments at 8 wpg and two experiments at 16 wpg.

observations were made for T cells in the lung and liver, with the exception of hepatic $CD4^+$ T cells that were decreased (Supporting Information Fig. 1A, B). Regulatory T cells (that have a $CD4^+CD127^-CD25^+$ phenotype) were equally rare in the spleen of 8 weeks postgraft BRGS and BRGSA2DR2 HIS mice (Supporting Information Fig. 3). In older animals, we detected a significant $CD127^-CD25^+$ T_{reg} population that included a previously described highly suppressive HLA $DR^+CD45RA^-$ subset [30] that was significantly increased in BRGSA2DR2 HIS mice (Supporting Information Fig. 3).

Concerning T-cell activation states, we observed significant increases in the percentages of $CD45RO^+$ $CD4^+$ T cells in the spleen, lung, and liver of BRGSA2DR2 HIS mice (Fig. 4C; Supporting Information Fig. 1A, C). In contrast, this was not the case for $CD8^+$ T cells in any tissue examined and this did not impact on the absolute numbers of $CD45RO^+$ $CD4^+$ and $CD8^+$ T cells when comparing BRGS and BRGSA2DR2 HIS mice (Fig. 4C, D; Supporting Information Fig. 1A, C). When comparing N, CM, EM, and EMRA T-cell subsets, we found that BRGSA2DR2 HIS mice showed a shift toward central memory T cells at the expense of naive T cells for both $CD4^+$ and $CD8^+$ T cells in the spleen, lung, and liver (Fig. 4E; Supporting Information Fig. 1B, D), consistently with a previous study [19].

$CD4^+$ and $CD8^+$ T cells in BRGSA2DR2 HIS mice have increased polyfunctionality

We next compared the functionality of mature splenic T cells in BRGS and BRGSA2DR2 HIS mice following exposure to pharmacological agents (PMA/ionomycin). As previously described in several different HIS mouse models, peripheral T cells can secrete

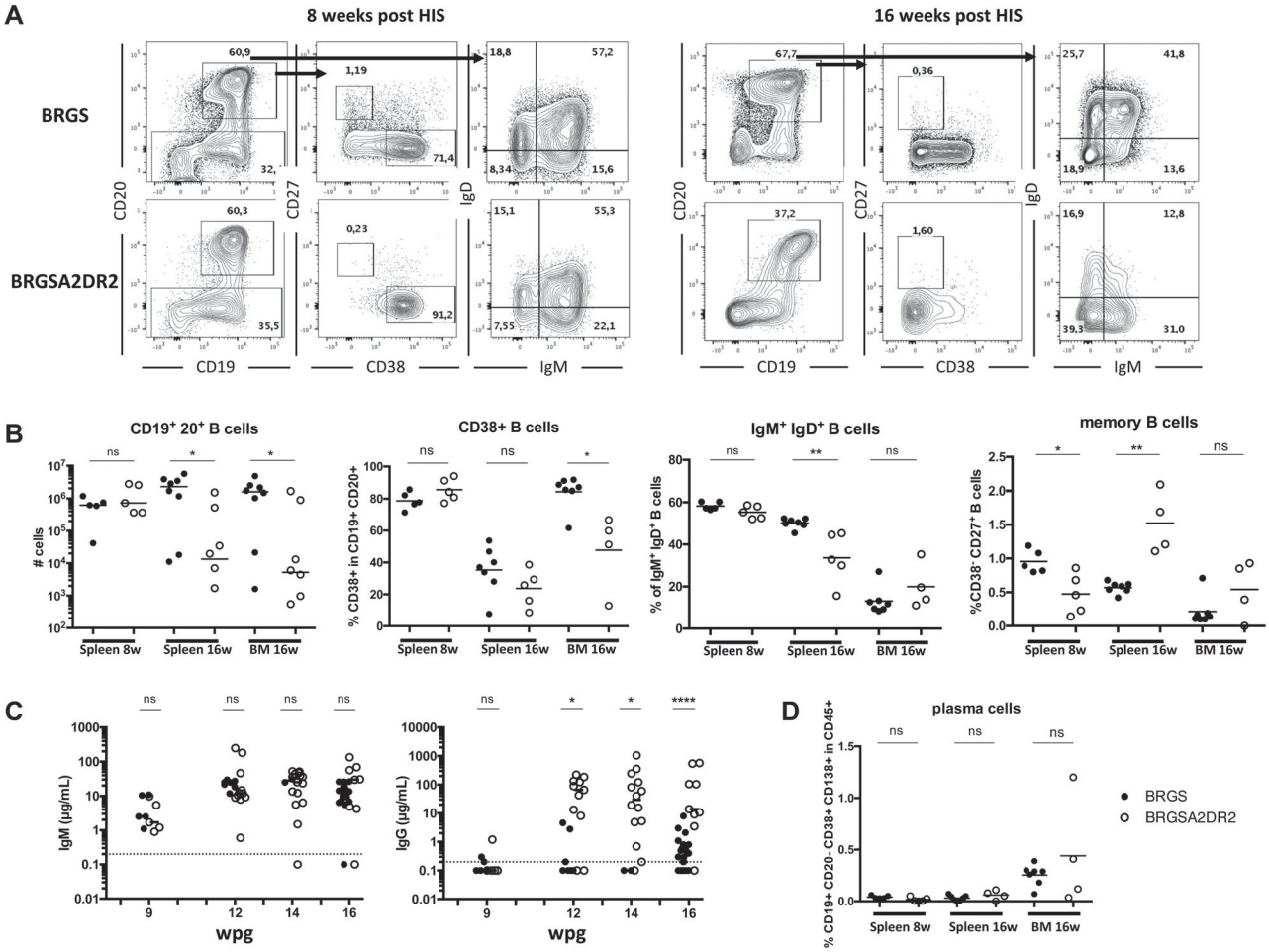

Figure 3. Human B-cell reconstitution in the lymphoid organs of BRGS versus BRGSA2DR2 HIS mice. (A) Representative flow cytometry and gating strategy for the mature/memory phenotype of B cells in the spleen within single, alive, hCD45$^+$, CD3$^-$ cells in both models at 8 and 16 wpg. (B) Absolute numbers of CD19$^+$CD20$^+$ B cells and frequency of mature IgM$^+$IgD$^+$, memory CD27$^+$CD38$^-$, immature (CD38$^+$ IgM$^+$ IgD$^-$C D10$^+$), and CD38$^+$ in CD19$^+$CD20$^+$ B cells for BRGS (full symbols) and BRGSA2DR2 (open symbols) mice at 8 (spleen) and 16 wpg (spleen and bone marrow). (C) Steady-state human immunoglobulin M (IgM) and G (IgG) titers in the plasma of BRGS (full circles) and BRGSA2DR2 (open circles) HIS mice between 8/9 wpg (pooled) and 16 wpg. (D) Absolute numbers of CD38$^+$CD138$^+$ plasma cells at 8 (spleen) and 16 wpg (spleen and bone marrow). Each dot represents one mouse and data are representative from three experiments at 8 wpg (five mice in each group) and two experiments at 16 wpg (7–8 mice in each group) for (A) and (B), with a threshold number of 10^4 cells for subsequent analysis of B-cell phenotype. For (C), each dot represents one mouse and data are pooled from at least five independent experiments (5–14 mice per group).

a range of cytokines following in vitro activation [11, 14, 17, 31]. This was the case for T cells in BRGS-based HIS mice that produced IFN-γ, TNF-α, and expressed the cytotoxic effector molecule granzyme B (Fig. 5A, B). When analyzing individual effectors, we found significant increases in the percentages of CD4$^+$ T cells expressing IFN-γ and CD8$^+$ T cells expressing granzyme B (Fig. 5A, B). The latter was in part due to a higher baseline level of granzyme B that was observed in both splenic CD4$^+$ and CD8$^+$ T cells in BRGSA2DR2 HIS mice. Regarding polyfunctional T cells, BRGSA2DR2 HIS mice showed increased percentages of both CD4$^+$ and CD8$^+$ T cells coexpressing two (IFN-γ, TNF-α) or three (IFN-γ, TNF-α, granzyme B) effector pathways (Fig. 5A, B; Supporting Information Fig. 2). Together, these results suggest that BRGSA2DR2 HIS mice have an enhanced capacity to generate multifunctional differentiated T cells.

MVA vaccinated BRGSA2DR2 HIS mice generate antigen-specific T- and B-cell responses

To evaluate the overall capacity of BRGSA2DR2 HIS mice to generate immune responses, we immunized animals using a single dose of a Modified Vaccinia virus Ankara vaccine (MVA-HIVB, French National Agency for AIDS Research ANRS) [32, 33] encoding a full-length Gag protein and as well as partial Pol and Nef antigens (Fig. 6A). Ten days after immunization, no major changes in T-cell subsets were observed in either BRGS or BRGSA2DR2 HIS mice suggesting minimal induction of T-cell activation or proliferation (Fig. 6B; Supporting Information Fig. 4). However critical differences were noted between the BRGS and BRGSA2DR2 models after immunization: we detected increased numbers of CD8$^+$ T cells and an increased frequency of effector memory

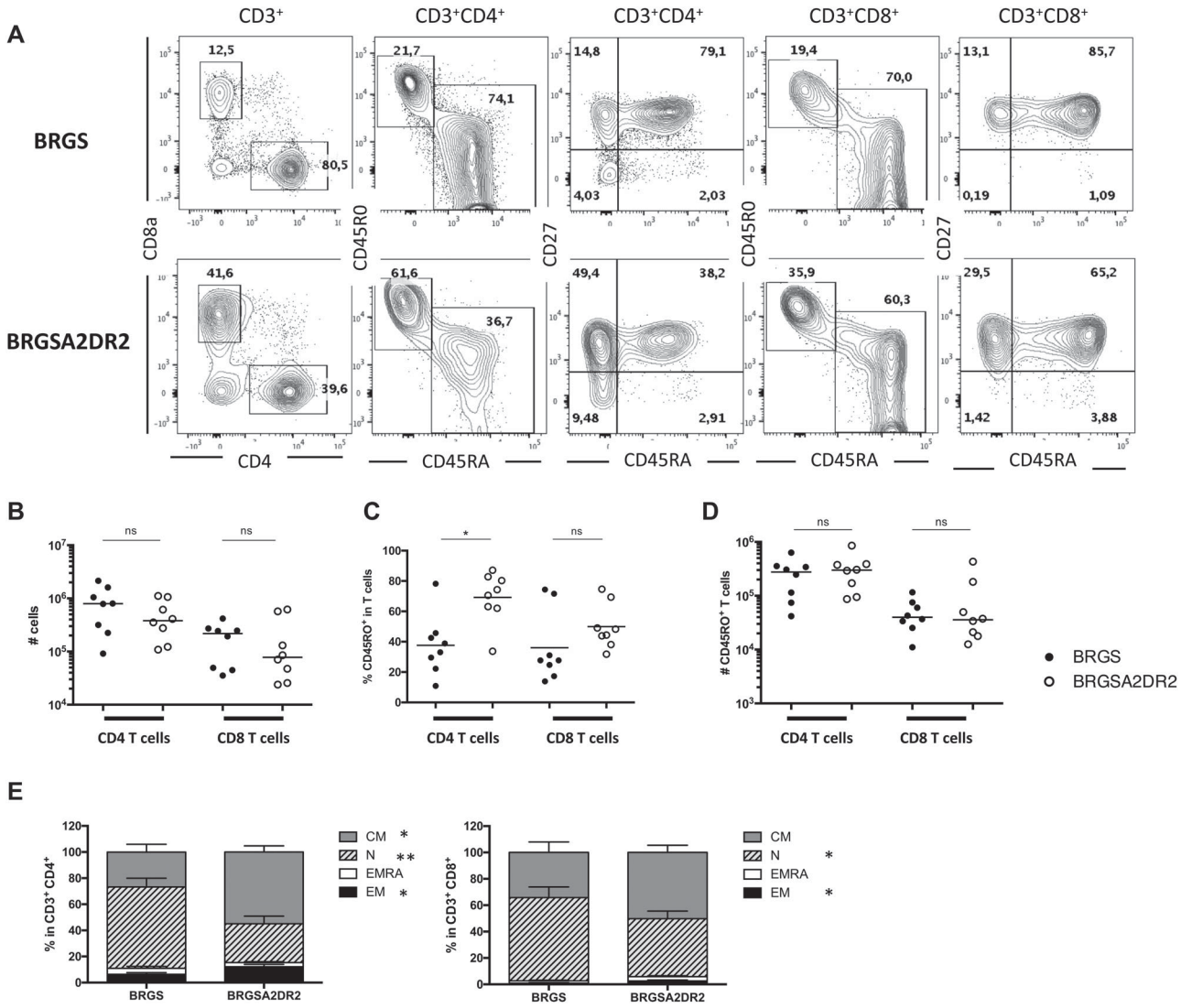

Figure 4. T-cell phenotype in BRGS versus BRGSA2DR2 HIS mice. (A) Representative flow cytometry and gating strategy for the activating/memory phenotype of T cells in the spleen within single, alive, hCD45$^+$, CD3$^+$ cells at 16 wpg. (B) Absolute numbers of CD4$^+$ and CD8$^+$ T cells in the spleen of BRGS (full symbols) and BRGSA2DR2 (open symbols) 16 wpg HIS mice reconstituted with HLA-A*02$^+$ HLA-DRB1*15$^+$ HSCs. Frequency (C) and absolute numbers (D) of activated/memory CD45RO$^+$ among CD4$^+$ and CD8$^+$ in the spleen of both models. (E) Bar graph showing relative frequencies of T-cell memory subsets in the spleen of BRGS and BRGSA2DR2 for CD4$^+$ (left panel) and CD8$^+$ (right panel) cells (N: naive CD45RA$^+$ CD27$^+$, CM: central memory CD45RA$^-$ CD27$^+$, EM: effector memory CD45RA$^-$ CD27$^-$, EMRA: Effector memory terminally differentiated CD45RA$^+$, CD27$^-$). Each dot represents one mouse. Representative data of seven to eight mice in each group from two independent experiments at 16 wpg. Statistical analysis (p-value summary) comparing the frequency of each subset from the two models are on the side of the bar graph legend.

population, especially for CD4$^+$ T cells (Fig. 6B). Importantly, T cell-specific responses were only detectable in BRGS A2DR2 HIS mice where we could observe a significant increase in Gag-specific T-cell responses (Fig. 6C). We further documented that three out of 12 MVA-HIVB immunized animals developed MVA-specific IgG responses in the plasma (Fig. 6D). These results suggest that interactions of human T cells with HLA molecules are critical for the differentiation of mature T cells that can respond in an antigen-specific fashion after immunization.

Discussion

Humanized mice engrafted with human HSC and reconstituted with a human immune system can be used to investigate the development of human immune cells in vivo. They also represent a new preclinical model for studying the physiopathology of human pathogens (reviewed in [34–37]) or the efficacy of therapeutic intervention or vaccines [38, 39]. However, the lack of HLA expression on murine thymic epithelium and in peripheral

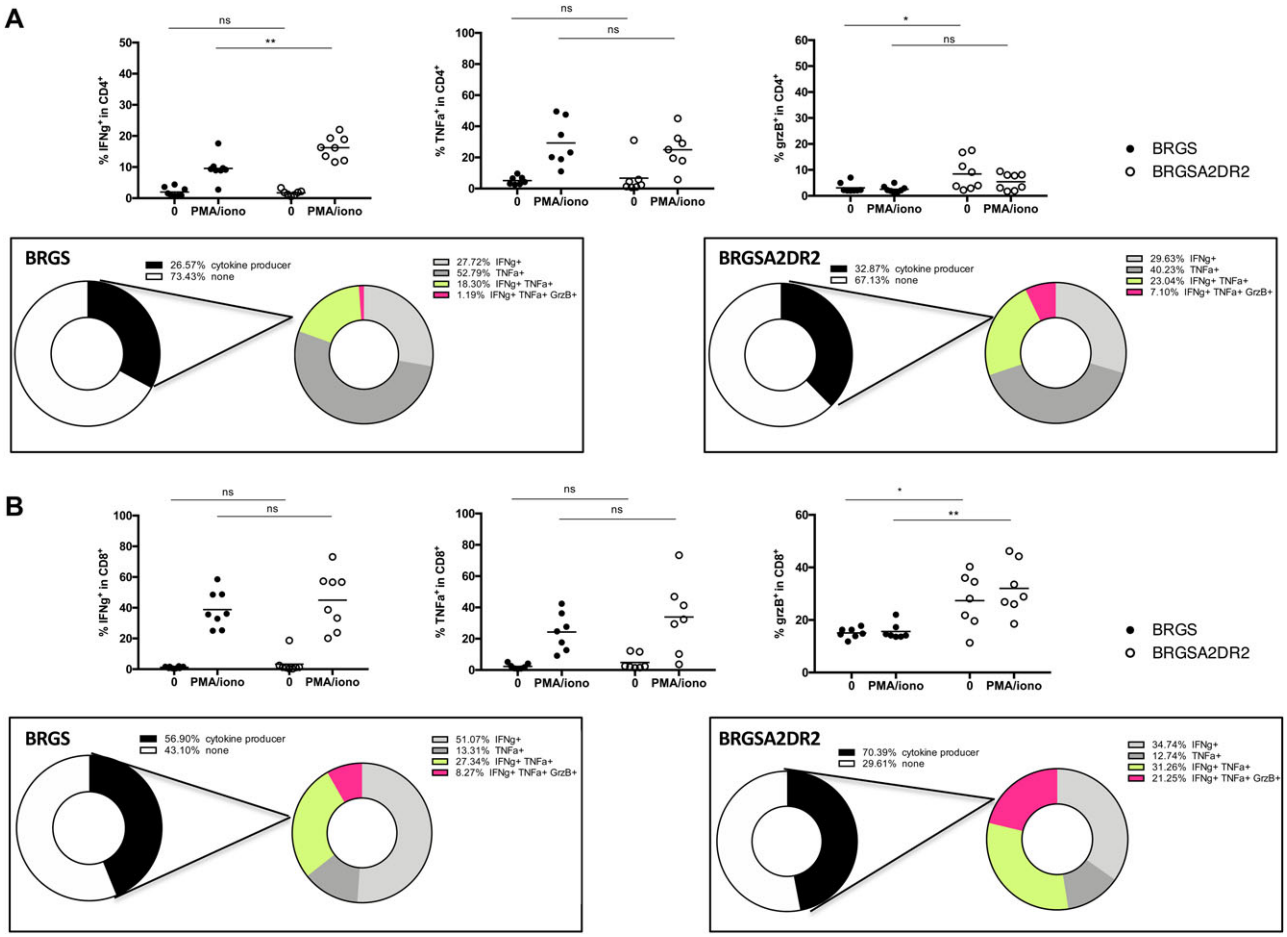

Figure 5. T-cell function in BRGS versus BRGSA2DR2 HIS mice. IFN-γ, TNF-α, and granzyme B expression by splenic CD4$^+$ and CD8$^+$ T cells following overnight stimulation in vitro. Splenic CD4$^+$ (A) and CD8$^+$ T cells (B) in BRGS (full symbols) and BRGSA2DR2 (open symbols) HIS mice at 16 wpg. The circular diagrams show the distribution of producing cells versus nonproducing (left diagram), and the different cytokine profiles in the producing cell gate (right diagram) (IFN-γ$^+$, TNF-α$^+$, IFN-γ$^+$ TNF-α$^+$, IFN-γ$^+$ TNF-α$^+$ GrzB$^+$) in BRGS and BRGSA2DR2 HIS mice. Low levels of IL-13 and IL-17 were also detected (data not shown). Representative data of seven to eight mice in each group from two independent experiments at 16 wpg.

tissues in most HIS mouse models may limit the extent of human T-cell development, education, and function, thereby reducing the capacity of these models to "read out" human cellular immune responses.

Considering the tight coevolution of T-cell receptors and MHC molecules, optimal human thymopoiesis and T-cell selection would necessitate the presence of human HLA on mouse thymic epithelial cells or the presence of human epithelial cells in the mouse thymus. Thymic epithelial cells promote selection of the "helper" CD4$^+$ and "cytotoxic" CD8$^+$ T cells via MHC class II and MHC class I, respectively. In the case of HIS mice, the MHC molecules that select human T cells from CD34$^+$ HSC precursors is assumed to be the corresponding murine H-2 homologs, although this has not been rigorously tested. While several immunodeficient NSG/NOG hosts lacking murine class I and/or class II molecules have been reported [40–42], only one study assessed the role for mouse MHC in human thymopoiesis in HIS mice [8]. These authors studied NOG mice lacking class II Ab sequences and found < 1% of CD4SP cells developed in the thymus of this HIS mouse model. Moreover, human T cells in the spleen of these HIS mice failed to proliferate in response to CD3 activation [8]. Although human T-cell signaling pathways were not extensively studied, this study suggests that mouse H-2A^b class II molecules are important for intrathymic selection of human CD4$^+$ T cells and for functional differentiation of both CD4$^+$ and CD8$^+$ T cells.

Several studies have reported the impact of enforced expression of HLA class I and/or class II molecules on human T-cell development in different HIS mouse models. The experimental approaches included HLA class I transgenes alone [10, 12–14], class II transgenes alone [11, 15, 19] or both class I and class II transgenes [20, 21]. Engraftment of "matched" CD34$^+$ HSC (meaning cells that bear the same allele as the transgenic HLA) was performed in some cases. In most cases, an enhancement of overall T-cell homeostasis and/or function can be noted, although the cellular mechanisms that account for these changes are not always clearly defined. For example, HLA-B*51:01 transgenic hosts improved overall thymopoiesis in the NOK (NOD/SCID/JAK3$^{-/-}$) background although matched

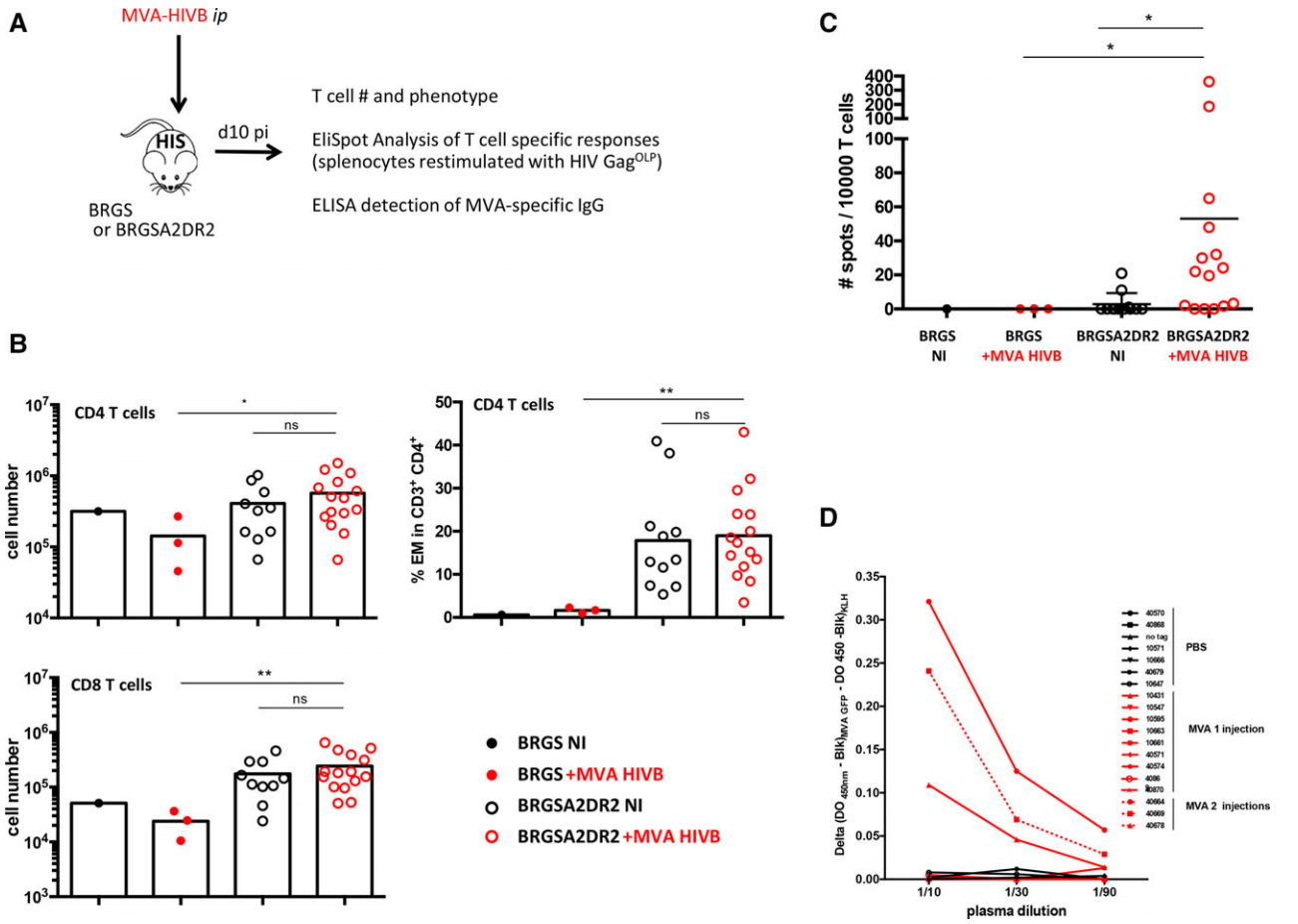

Figure 6. Antigen-specific HIV responses in BRGS versus BRGSA2DR2 mice. (A) Schematic overview of the MVA-HIVB immunization of HIS mice between 12 and 16 wpg. (B) Splenic CD4$^+$ and CD8$^+$ T cells numbers in nonimmunized (black symbols) and immunized (red symbols) from BRGS (full symbols) and BRGSA2DR2 (open symbols) HIS mice. (C) ELISPOT IFN-γ analysis of splenocytes from BRGS (full circles) and BRGSA2DR2 (open circles) reconstituted with HLA-A*02$^+$ HLA-DRB1*15$^+$ HSCs 10 days after immunization with MVA-HIV^{GPN} viral particles (red symbols). (D) MVA vector-specific IgG response in the plasma determined by ELISA from MVA-HIVB immunized and nonimmunized BRGSA2DR2 HIS mice. Nonimmunized BRGS and BRGSA2DR2 animals were also analyzed as controls (black circles). Each dot represents one mouse. Representative data of three independent experiments with one (BRGS NI) to seven mice analyzed per group.

HLA-B51$^+$ HSC were not used [13]. In contrast, Suzuki et al. demonstrated that engraftment of HLA-DR matched HSCs are critical for T- and B-cell function in humanized HLA DR4 NOG transgenic mice as HIS mice made using mismatched HSCs could not produce IgG after OVA immunization [15].

In this report, we analyzed the impact of HLA class I and class II transgenes on human T-cell development and function in the Balb/c *Rag2*$^{-/-}$ *Il2rg*$^{-/-}$ *Sirpa*^{NOD} (BRGS) HIS model [2, 22, 23]. Several different HIS models exist: all are based on immunodeficient mice (Rag2/Il2rg DKO, SCID/Il2rg DKO) that harbor SIRPa polymorphisms from the NOD background as has been reviewed extensively [6]. Compared to NSG-based HIS mice, BRGS-based HIS mice show very similar human cell reconstitution (Legrand et al. 2011) but do not exhibit irradiation sensitivity that characterizes SCID-based HIS models. As such, the Rag-based HIS models (including BRGS) may be less subjected to spontaneous mortality or graft-versus-host disease development upon human cell reconstitution compared with SCID-based counterparts.

Human immune cell reconstitution using HLA transgenic BRGS hosts was compared with nontransgenic BRGS recipients using the same CD34$^+$ HSC donor cells that expressed HLA-A2 and HLA-DR2. We observed that matching for donor HSC accelerated overall lymphoid reconstitution, resulting in balanced B/T-cell development and improved peripheral lymphocyte functionality. In particular, BRGSA2DR2 HIS mice were highly responsive to the MVA-based HIV vaccine (MVA-HIVB, French National Agency for AIDS Research ANRS) [32, 33] demonstrating their capacity to generate antigen-specific T-cell responses following immunization. Moreover, BRGS HIS animals are healthy and do not develop any signs of autoimmune or inflammatory disease.

Previous studies compared the DRAGA NRG-based HIS model (bearing HLA-A2 class I and HLA-DR4 class II transgenes) to the single HLA-A2 class I and to the single HLA-DR4 transgenic NRG mice [21]. Interestingly, the DR4 transgene appeared to make a larger contribution to the improvement in overall performance of their model (thymic engraftment, frequency of mice with human reconstitution, number of CD4 cells, immunoglobulin class

switching, cytokine secretion, CD8 cytotoxicity) compared to the HLA-A2 transgene, with DRAGA HIS mice showing a similar phenotype to the DR4 single transgenics. Similarly, the frequency of CD4 CM T cells are increased in NSG-based HIS mice that express DR1 using AAV [19]. Other reports showed a major contribution of the HLA-A2 transgene to overall T-cell development and differentiation [13, 14]. Interestingly, EBV-infected NSG HLA-A2 transgenic mouse splenocytes showed a high capacity to respond to EBV dominant antigens, whereas NSG mice did not, and tetramer detection of specific $CD8^+$ T cells became possible [17].

While we have not extensively compared single HLA-A2 versus HLA-DR2 BRGS HIS mice, our preliminary experiments indicate that MVA-induced immune responses can be elicited in HLA-A2 only BRGS HIS mice. Further studies will be necessary to understand how expression of class I or class II HLA impacts on human T-cell differentiation in our HIS mouse model.

Several studies have reported an immature phenotype of B cells in humanized mouse models [8, 43–46]. The reconstitution of functional B cells is also reported to be limited in patients that receive cord blood HSCs [47]. However, it seems clear that the engrafted human hematopoietic systems in HIS mice evolves with time, with an increase in mature B-cell generation as animals age and accumulate activated T cells [4]. Our data suggest that improved development of T cells in HLA transgenic mice might increase B-cell differentiation and the steady state IgG levels by a similar mechanism.

Taken together, our results suggest that BRGSA2DR2 HIS mice provide an improved model to assess human immune responses to pathogens or vaccines in vivo. As recent modifications to the BRGS model have generated HIS mice with enhanced DC function (BRGSF; [16]) or robust LN development (BRGST; [18]), it will be interesting to assess the impact of human HLA expression on human immune function in HIS mice that combine these different modifications.

Materials and methods

Ethics statement

Animals were housed in micro-isolators under pathogen-free conditions with humane care. Experiments were approved by an institutional ethical committee at the Institut Pasteur and validated by the French Ministry of Education and Research (Reference MENESR # 02162.01).

Mice

HLA-A*02-HHD class I and HLA-DRB1*15 class II transgenic mice [22, 23] have been backcrossed (>10 generations) to the Balb/c *Rag2*$^{-/-}$ *Il2rg*$^{-/-}$ *Sirpa*^{NOD} strain (BRGS) [2] to create BRGSA2DR2 hosts.

Generation of HIS mice

BRGS and BRGSA2DR2 mice were used as recipients to create HIS mice as previously described [16, 18, 24, 25, 27]. Briefly, fetal liver $CD34^+$ cells were isolated using affinity matrices according to manufacturer's instructions (Miltenyi Biotec) and subsequently phenotyped for CD34, CD38, and HLA-A2 expression by FACS (Supporting Information Table 1). Dry pellets of CD34-negative fractions were haplotyped for HLA class I and class II alleles by PCR (LABType SSO, One Lambda). Newborn (3–5 day old) pups were sublethally irradiated (3 Gy) and injected intrahepatically with 5 to 10×10^4 $CD34^+CD38^-$ human fetal liver cells that were from HLA-A*02^+HLA-DRB1*15^+ donors or from 1:1 mixtures of HLA-A*02^+ and HLA-DRB1*15^+ donors. These two conditions generated similar immune reconstitution and immune responses to vaccination, and the same donor cells were always compared directly in BRGS and BRGSA2DR2 recipients. Analyses were performed on 8–16-week-old mice. All manipulations of HIS mice were performed under laminar flow conditions.

Cell isolation

Thymus and spleen were minced and filtered through 100 μm cell strainer (Falcon). Femur and tibia bones were crushed with mortar and pestle to extract cells. Lungs were cut into pieces before collagenase D digestion (Roche) for 45 min. Livers were minced using metallic filters. Percoll density gradient centrifugation (GE Healthcare Life Sciences) was used for liver and lung lymphocyte preparation. Erythrocytes were lysed using RBC lysing buffer Hybri-Max (Sigma). All cell preparation steps were performed using RPMI 1640 Glutamax (Life Technologies) supplemented with 100 U/mL penicillin, 100 g/mL streptomycin (Invitrogen), and 2% fetal calf serum.

Flow cytometry

For blood cells, the total percentage of hCD45 was determined using the formula hCD45%x100/(hCD45%+mCD45%). For organ-derived cells, fixable viability dye eFlour506 (ebioscience) was used to exclude dead cells and human and mouse FcR were blocked (polyclonal human IgG and 2.4G2 anti mouse Fc receptors) before antibody (Ab) staining. Fluorochrome-conjugated Abs from BD biosciences, Biolegend, ebioscience, and Miltenyi were used in this study (Supporting Information Table 1). For surface marker staining, cells were incubated with Abs on ice for 30 min. For intracellular cytokine detection, freshly isolated cells were stimulated with 50 ng/mL PMA (Sigma-Aldrich) and 1 μg/mL ionomycin (Sigma-Aldrich) for 4 hours in the presence of Golgi-plug (BD biosciences) (three last hours of stimulation) prior to intracellular cytokine staining using the BD cytofix/cytoperm kit (BD biosciences). Flow cytometers Fortessa (BD biosciences) or LSR II (BD biosciences) were used to acquire the data and Flowjo software (TreeStar) was used for data analysis. FACS acquisition

and analysis have been done according to the guidelines reported in [48].

Immunoglobulin titration

Human IgM and IgG levels were quantified by ELISA in the plasma as described [28]. MVA vector-specific IgG level were evaluated by ELISA using MVA-GFP coating (provided by the Vaccine Research Institute, Créteil) and plasma from immunized animals.

MVA-HIVB ^{GPN} vaccine immunization

Recombinant MVA expressing an HIV polyprotein (containing full-length Gag, fused to 3 Pol and 2 Nef fragments) was previously described [32] and provided by the Vaccine Research Institute, Créteil. The vaccine was injected by intraperitoneal (*ip*) route at the dose of 0.48 × 10exp7 pfu.

ELISPOT assay

The 96-well plates with a nitrocellulose filter base (MultiScreen, Millipore) were coated with purified anti–IFN-γ capture antibodies (human IFN-γ ELISPOT pair, BD biosciences). After overnight incubation at 4°C, the plates were washed twice with glutamine containing IMDM (Lonza), 10% FCS and penicillin/streptomycin (Gibco) and incubated for 2 hours at room temperature for the blocking step. Splenocytes were added to the plates in doubling dilutions from 5×10^5 cells per well in the presence of 100 μg/mL overlapping peptide pool from the HIV Gag full-length protein (final concentration 1 μg/mL for each peptide in the plate) and 1 μg/mL purified anti-CD28 (clone 28.2, eBioscience) or anti-human CD3/CD28 activating beads (Dynabeads, Gibco) for restimulation, both in the presence of IL-2 (10 IU/mL) and IL-7 (100 ng/mL) (Miltenyi Biotech). Doubling dilutions were also applied to nonstimulated splenocytes (only maintained in IL-2 and IL-7) to determine the background. After 36 h incubation in a 37°C 5% CO_2 incubator, the plates were washed following the manufacturer's protocol (human IFN-γ ELISPOT pair, BD biosciences), incubated with biotinylated anti-IFN-γ detection antibody (BD Biosciences), followed by streptavidin-HRP conjugate (BD Biosciences), and the AEC substrate kit (BD Biosciences). The plates were then dried and the red spots were enumerated using an ELISPOT counter (Bioreader 5000 Eb, Biosys).

Statistical analysis

Datasets were tested with two-tailed unpaired non-parametric Mann–Whitney tests, using Prism version 6 (GraphPad Software). Significant p values are shown as: $^*p < 0.05$, $^{**}p < 0.005$, $^{***}p < 0.0005$. Lines showing the means in each data set were applied in linear scale graphs, whereas medians were applied for logarithmic scale graphs.

Acknowledgments: The authors thank the Center for Translational Research, the Cytometry and Biomarkers UTechS (CBUTechS, Institut Pasteur) and the Animalerie Centrale of Institut Pasteur for collaboration and N. Court, N. Huntington, and J.-J. Mention for their help during the early phases of this work. Supported by grants from the Institut Pasteur, INSERM, Gates Foundation (Grand Challenges in Global Health; J.P.D.), Agence Nationale de la Recherche (ANR) programme RPIB (Im_HIS; J.P.D.), the Laboratoire d'Excellence REVIVE (ANR-10-LABX-73; J.P.D.), the Laboratoire d'Excellence Vaccine Research Institute (ANR-10-LABX-77; Y.L.), the Laboratoire d'Excellence *Milieu Intérieur* (ANR-10-LABX-69; H.M.), the Laboratoire d'Excellence IBEID (ANR-10-LABX-62; O.S.), the Agence Nationale de Recherche sur le SIDA et les hepatites virales (ANRS 15465; O.S.), the European Commission Seventh Framework Programme n°305578 (PathCO; J.P.D.), and Gilead Sciences (00397; O.S. and J.P.D.).

Conflict of interest: N.L. and E.C. are employed by genOway. H.S. is employee of AIMM Therapeutics. The remaining authors declare no competing interests.

References

1 **Ishikawa, F., Yasukawa, M., Lyons, B., Yoshida, S., Miyamoto, T., Yoshimoto, G., Watanabe, T. et al.**, Development of functional human blood and immune systems in NOD/SCID/IL2 receptor {gamma} chain(null) mice. *Blood* 2005. **106**: 1565–1573.

2 **Legrand, N., Huntington, N. D., Nagasawa, M., Bakker, A. Q., Schotte, R., Strick-Marchand, H., de Geus, S. J. et al.**, Functional CD47/signal regulatory protein alpha (SIRP(alpha)) interaction is required for optimal human T- and natural killer- (NK) cell homeostasis in vivo. *Proc. Natl. Acad. Sci. USA* 2011. **108**: 13224–13229.

3 **Traggiai, E., Chicha, L., Mazzucchelli, L., Bronz, L., Piffaretti, J.-C., Lanzavecchia, A. and Manz, M. G.**, Development of a human adaptive immune system in cord blood cell-transplanted mice. *Science* 2004. **304**: 104–107.

4 **Lang, J., Kelly, M., Freed, B. M., McCarter, M. D., Kedl, R. M., Torres, R. M. and Pelanda, R.**, Studies of lymphocyte reconstitution in a humanized mouse model reveal a requirement of T cells for human B cell maturation. *J. Immunol. Baltim. Md 1950.* 2013. **190**: 2090–2101.

5 **Patton, J., Vuyyuru, R., Siglin, A., Root, M. and Manser, T.**, Evaluation of the efficiency of human immune system reconstitution in NSG mice and NSG mice containing a human HLA.A2 transgene using hematopoietic stem cells purified from different sources. *J. Immunol. Methods* 2015. **422**: 13–21.

6 **Shultz, L. D., Brehm, M. A., Garcia-Martinez, J. V. and Greiner, D. L.**, Humanized mice for immune system investigation: progress, promise and challenges. *Nat. Rev. Immunol.* 2012. **12**: 786–798.

7 **Sato, Y., Takata, H., Kobayashi, N., Nagata, S., Nakagata, N., Ueno, T. and Takiguchi, M.**, Failure of effector function of human CD8+ T Cells in NOD/SCID/JAK3^{-}/$^{-}$ immunodeficient mice transplanted with human CD34+ hematopoietic stem cells. *PloS One* 2010. **5**: e13109.

8 **Watanabe, Y., Takahashi, T., Okajima, A., Shiokawa, M., Ishii, N., Katano, I., Ito, R. et al.**, The analysis of the functions of human B and T cells in humanized NOD/shi-scid/gammac(null) (NOG) mice (hu-HSC NOG mice). *Int. Immunol.* 2009. **21**: 843–858.

9 **Becker, P. D., Legrand, N., van Geelen, C. M. M., Noerder, M., Huntington, N. D., Lim, A., Yasuda, E. et al.**, Generation of human antigen-specific monoclonal IgM antibodies using vaccinated 'human immune system' mice. *PloS One* 2010. **5**: e13137.

10 **Billerbeck, E., Horwitz, J. A., Labitt, R. N., Donovan, B. M., Vega, K., Budell, W. C., Koo, G. C. et al.**, Characterization of human antiviral adaptive immune responses during hepatotropic virus infection in HLA-transgenic human immune system mice. *J. Immunol. Baltim. Md 1950.* 2013. **191**: 1753–1764.

11 **Danner, R., Chaudhari, S. N., Rosenberger, J., Surls, J., Richie, T. L., Brumeanu, T.-D. and Casares, S.**, Expression of HLA class II molecules in humanized NOD.Rag1KO.IL2RgcKO mice is critical for development and function of human T and B cells. *PloS One* 2011. **6**: e19826.

12 **Jaiswal, S., Pearson, T., Friberg, H., Shultz, L. D., Greiner, D. L., Rothman, A. L. and Mathew, A.**, Dengue virus infection and virus-specific HLA-A2 restricted immune responses in humanized NOD-scid IL2rgammanull mice. *PloS One* 2009. **4**: e7251.

13 **Sato, Y., Nagata, S. and Takiguchi, M.**, Effective elicitation of human effector CD8+ T Cells in HLA-B*51:01 transgenic humanized mice after infection with HIV-1. *PloS One* 2012. **7**: e42776.

14 **Shultz, L. D., Saito, Y., Najima, Y., Tanaka, S., Ochi, T., Tomizawa, M., Doi, T. et al.**, Generation of functional human T-cell subsets with HLA-restricted immune responses in HLA class I expressing NOD/SCID/IL2r gamma(null) humanized mice. *Proc. Natl. Acad. Sci. USA* 2010. **107**: 13022–13027.

15 **Suzuki, M., Takahashi, T., Katano, I., Ito, R., Ito, M., Harigae, H., Ishii, N. et al.**, Induction of human humoral immune responses in a novel HLA-DR-expressing transgenic NOD/Shi-scid/γcnull mouse. *Int. Immunol.* 2012. **24**: 243–252.

16 **Li, Y., Mention, J.-J., Court, N., Masse-Ranson, G., Toubert, A., Spits, H., Legrand, N. et al.**, A novel Flt3-deficient HIS mouse model with selective enhancement of human DC development. *Eur. J. Immunol.* 2016. **46**: 1291–1299.

17 **Strowig, T., Gurer, C., Ploss, A., Liu, Y.-F., Arrey, F., Sashihara, J., Koo, G. et al.**, Priming of protective T cell responses against virus-induced tumors in mice with human immune system components. *J. Exp. Med.* 2009. **206**: 1423–1434.

18 **Li, Y., Masse-Ranson, G., Garcia, Z., Bruel, T., Kök, A., Strick-Marchand, H., Jouvion, G. et al.**, A human immune system mouse model with robust lymph node development. *Nat. Methods* 2018. **15**: 623–630.

19 **Huang, J., Li, X., Coelho-dos-Reis, J. G. A., Zhang, M., Mitchell, R., Nogueira, R. T., Tsao, T. et al.**, Human immune system mice immunized with *Plasmodium falciparum* circumsporozoite protein induce protective human humoral immunity against malaria. *J. Immunol. Methods* 2015. **427**: 42–50.

20 **Mendoza, M., Ballesteros, A., Qiu, Q., Pow Sang, L., Shashikumar, S., Casares, S. and Brumeanu, T.-D.**, Generation and testing anti-influenza human monoclonal antibodies in a new humanized mouse model (DRAGA: HLA-A2. HLA-DR4. Rag1 KO. IL-2Rγc KO. NOD). *Hum. Vaccines Immunother.* 2018. **14**: 345–360.

21 **Majji, S., Wijayalath, W., Shashikumar, S., Pow-Sang, L., Villasante, E., Brumeanu, T. D. and Casares, S.**, Differential effect of HLA class-I versus class-II transgenes on human T and B cell reconstitution and function in NRG mice. *Sci. Rep.* 2016. **6**: 28093.

22 **Pascolo, S., Bervas, N., Ure, J. M., Smith, A. G., Lemonnier, F. A. and Pérarnau, B.**, HLA-A2.1-restricted education and cytolytic activity of CD8(+) T lymphocytes from beta2 microglobulin (beta2m) HLA-A2.1 monochain transgenic H-2Db beta2m double knockout mice. *J. Exp. Med.* 1997. **185**: 2043–2051.

23 **Madsen, L. S., Andersson, E. C., Jansson, L., krogsgaard, M., Andersen, C. B., Engberg, J., Strominger, J. L. et al.**, A humanized model for multiple sclerosis using HLA-DR2 and a human T-cell receptor. *Nat. Genet.* 1999. **23**: 343–347.

24 **Dusséaux, M., Masse-Ranson, G., Darche, S., Ahodantin, J., Li, Y., Fiquet, O., Beaumont, E. et al.**, Viral load affects the immune response to HBV in mice with humanized immune system and liver. *Gastroenterology* 2017. **153**: 1647–1661.e9.

25 **Huntington, N. D., Alves, N. L., Legrand, N., Lim, A., Strick-Marchand, H., Mention, J.-J., Plet, A. et al.**, IL-15 transpresentation promotes both human T-cell reconstitution and T-cell-dependent antibody responses in vivo. *Proc. Natl. Acad. Sci. USA* 2011. **108**: 6217–6222.

26 **Lim, A. I., Li, Y., Lopez-Lastra, S., Stadhouders, R., Paul, F., Casrouge, A., Serafini, N. et al.**, Systemic human ILC precursors provide a substrate for tissue ILC differentiation. *Cell* 2017. **168**: 1086–1100.e10.

27 **Lopez-Lastra, S., Masse-Ranson, G., Fiquet, O., Darche, S., Serafini, N., Li, Y., Dusséaux, M. et al.**, A functional DC cross talk promotes human ILC homeostasis in humanized mice. *Blood Adv.* 2017. **1**: 601–614.

28 **Strick-Marchand, H., Dusséaux, M., Darche, S., Huntington, N. D., Legrand, N., Masse-Ranson, G., Corcuff, E. et al.**, A novel mouse model for stable engraftment of a human immune system and human hepatocytes. *PloS One* 2015. **10**: e0119820.

29 **Yu, H., Borsotti, C., Schickel, J.-N., Zhu, S., Strowig, T., Eynon, E. E., Frleta, D. et al.**, A novel humanized mouse model with significant improvement of class-switched, antigen-specific antibody production. *Blood* 2017. **129**: 959–969.

30 **Schaier, M., Seissler, N., Schmitt, E., Meuer, S., Hug, F., Zeier, M. and Steinborn, A.**, DR(high+)CD45RA(-)-Tregs potentially affect the suppressive activity of the total Treg pool in renal transplant patients. *PloS One* 2012. **7**: e34208.

31 **Brainard, D. M., Seung, E., Frahm, N., Cariappa, A., Bailey, C. C., Hart, W. K., Shin, H.-S. et al.**, Induction of robust cellular and humoral virus-specific adaptive immune responses in human immunodeficiency virus-infected humanized BLT mice. *J. Virol.* 2009. **83**: 7305–7321.

32 **Brandler, S., Lepelley, A., Desdouits, M., Guivel-Benhassine, F., Ceccaldi, P.-E., Lévy, Y., Schwartz, O. et al.**, Preclinical studies of a modified vaccinia virus Ankara-based HIV candidate vaccine: antigen presentation and antiviral effect. *J. Virol.* 2010. **84**: 5314–5328.

33 **Garcia, Z., Lemaître, F., van Rooijen, N., Albert, M. L., Levy, Y., Schwartz, O. and Bousso, P.**, Subcapsular sinus macrophages promote NK cell accumulation and activation in response to lymph-borne viral particles. *Blood* 2012. **120**: 4744–4750.

34 **Douam, F. and Ploss, A.**, The use of humanized mice for studies of viral pathogenesis and immunity. *Curr. Opin. Virol.* 2018. **29**: 62–71.

35 **Kremsdorf, D. and Strick-Marchand, H.**, Modeling hepatitis virus infections and treatment strategies in humanized mice. *Curr. Opin. Virol.* 2017. **25**: 119–125.

36 **Masse-Ranson, G., Mouquet, H. and Di Santo, J. P.**, Humanized mouse models to study pathophysiology and treatment of HIV infection. *Curr. Opin. HIV AIDS* 2018. **13**: 143–151.

37 **Münz, C.**, Humanized mouse models for Epstein Barr virus infection. *Curr. Opin. Virol.* 2017. **25**: 113–118.

38 **Centlivre, M. and Combadière, B.**, New challenges in modern vaccinology. *BMC Immunol.* 2015. **16**: 18.

39 **West, A. P., Scharf, L., Scheid, J. F., Klein, F., Bjorkman, P. J. and Nussenzweig, M. C.**, Structural insights on the role of antibodies in HIV-1 vaccine and therapy. *Cell* 2014. **156**: 633–648.

40 **Gopalakrishnapillai, A., Kolb, E. A., Dhanan, P., Bojja, A. S., Mason, R. W., Corao, D. and Barwe, S. P.**, Generation of pediatric leukemia xenograft models in NSG-B2m mice: comparison with NOD/SCID mice. *Front. Oncol.* 2016. **6**: 162.

41 **King, M. A., Covassin, L., Brehm, M. A., Racki, W., Pearson, T., Leif, J., Laning, J. et al.**, Human peripheral blood leucocyte non-obese diabetic-severe combined immunodeficiency interleukin-2 receptor gamma chain gene mouse model of xenogeneic graft-versus-host-like disease and the role of host major histocompatibility complex. *Clin. Exp. Immunol.* 2009. **157**: 104–118.

42 **Pino, S., Brehm, M. A., Covassin-Barberis, L., King, M., Chase, T. H., Wagner, J., Burzenski, L. et al.**, Development of novel major histocompatibility complex class I and class II-deficient NOD-SCID IL2R gamma chain knockout mice for modeling human xenogeneic graft-versus-host disease. *Methods Mol. Biol.* 2010. **602**: 105–117.

43 **Biswas, S., Chang, H., Sarkis, P. T. N., Fikrig, E., Zhu, Q. and Marasco, W. A.**, Humoral immune responses in humanized BLT mice immunized with West Nile virus and HIV-1 envelope proteins are largely mediated via human CD5+ B cells. *Immunology* 2011. **134**: 419–433.

44 **Matsumura, T., Kametani, Y., Ando, K., Hirano, Y., Katano, I., Ito, R., Shiina, M. et al.**, Functional CD5+ B cells develop predominantly in the spleen of NOD/SCID/gammac(null) (NOG) mice transplanted either with human umbilical cord blood, bone marrow, or mobilized peripheral blood CD34+ cells. *Exp. Hematol.* 2003. **31**: 789–797.

45 **Vuyyuru, R., Patton, J. and Manser, T.**, Human immune system mice: current potential and limitations for translational research on human antibody responses. *Immunol. Res.* 2011. **51**: 257–266.

46 **Villaudy, J., Schotte, R., Legrand, N. and Spits, H.**, Critical assessment of human antibody generation in humanized mouse models. *J. Immunol. Methods* 2014. **410**: 18–27.

47 **Chiesa, R., Gilmour, K., Qasim, W., Adams, S., Worth, A. J. J., Zhan, H., Montiel-Equihua, C. A. et al.**, Omission of in vivo T-cell depletion promotes rapid expansion of naïve CD4+ cord blood lymphocytes and restores adaptive immunity within 2 months after unrelated cord blood transplant. *Br. J. Haematol.* 2012. **156**: 656–666.

48 **Cossarizza, A., Chang, H.-D., Radbruch, A., Akdis, M., Andrä, I., Annunziato, F., Bacher, P. et al.**, Guidelines for the use of flow cytometry and cell sorting in immunological studies. *Eur. J. Immunol.* 2017. **47**: 1584–1797.

Abbreviations: **CM**: central memory · **EM**: effector memory · **HIS**: human immune system · **HSC**: hematopoietic stem cell · **MVA**: modified vaccinia virus Ankara

Full correspondence: Prof. James P. Di Santo, Innate Immunity Unit, Inserm U1223, Institut Pasteur, 25 rue du Docteur Roux, 75724 Paris, France
e-mail: james.di-santo@pasteur.fr

The peer review history for this article is available at https://publons.com/publon/10.1002/eji.201848001

Received: 8/11/2018
Revised: 4/2/2019
Accepted: 4/3/2019
Accepted article online: 19/3/2019